Chapter 7
Comparison of Data-Driven Techniques for Structural Dynamics Model Order Reduction

Celso T. do Cabo, Yujie Xi, Raymond Joshua, and Zhu Mao

Abstract The vibrational behavior of structures is oftentimes used to define their state awareness and can be further employed for damage detection and prognosis. However, most structures have a complex behavior that cannot be easily interpreted or directly applied for damage detection. While many methods can be employed to model those systems, such as finite element models (FEM), these models depend on a strong understanding of physics as prior knowledge. With the increased number of monitoring systems and data availability for structural dynamics, data-driven technologies are becoming increasingly more popular for a variety of problems. Among unsupervised learning methods, dimension reduction techniques are widely used to simplify high-dimensional datasets. In addition, for linear models, Principal Component Analysis (PCA) or Proper Orthogonal Decomposition (POD) are some of the most known methods, which consists of employing Singular Value Decomposition (SVD) or eigen decomposition in the dataset itself. Furthermore, other techniques have been developed specifically for time-series applications, such as Dynamic Mode Decomposition (DMD). This work focuses on the comparison between the performance of data-driven dimension reduction techniques, such as the ones mentioned previously, as well as other improved versions of such technologies, such as optimized DMD when applied to structural dynamics. Different techniques are implemented and compared to the context of structural vibrations, and all techniques are compared with respect to their advantages and limitations, as well as the corresponding mathematical investigation.

Keywords Model Order Reduction · Structural Dynamics · Principal Component Analysis · Dynamic Mode Decomposition

Introduction

Vibrational behavior of structures is of critical importance for a variety of applications, such as to define its state awareness which can be further employed for damage detection and prognosis. However, their dynamical behavior oftentimes has a high complexity, which makes it difficult to interpret or directly employ for damage detection. While many methods can be applied to model dynamical systems, such as finite element models (FEM), these models depend on strong understanding of the physics as prior knowledge. With the increasing in data availability for structural dynamics, data-driven technologies are becoming increasingly more popular for a variety of applications. Among unsupervised methods, Principal Component Analysis (PCA) is a very well-known dimension reduction technique, which uses Singular Value Decomposition (SVD) to decompose the dataset into a different basis and reduce its order for simplification [1, 2]. In addition, Proper Orthogonal Decomposition (POD) works in a similar manner as PCA using SVD to decompose physical measurements and are often compared on how they are computed [3–5]. Such techniques were also previously employed into vibrational systems as a manner to reduce the order of the system, as well as to decompose the original signals into different modes [6–8].

NSC-614-5662 10/2024
Unclassified Unlimited Release

Celso T. do Cabo · Yujie Xi · Zhu Mao (✉)
Department of Mechanical and Materials Engineering, Worcester Polytechnic Institute, Worcester, MA 01609
e-mail: ctdocabo@wpi.edu; yxi@wpi.edu; zmao2@wpi.edu

Raymond Joshua
Honeywell Federal Manufacturing & Technologies, LLC operates the Kansas City, National Security Campus for the United States Department of Energy / National Nuclear
Security Administration under Contract Number DE-NA0002839
e-mail: rjoshua@kcnsc.doe.gov

© The Author(s), under exclusive license to River Publishers 2025

Brandon Dilworth et al. (eds.), *Topics in Modal Analysis & Parameter Identification I, Vol. 9*, Conference Proceedings of the Society for Experimental Mechanics Series, https://doi.org/10.13052/97887-438-0154-2_7

However, among dimension reduction techniques, more techniques have been developed specifically for physical problems, such as the Dynamic Mode Decomposition (DMD), which was developed specifically for time-series applications, initially being applied into fluid dynamics problems [9–11]. The technique uses the Koopman operator to obtain an approximate matrix which is time invariant, later applying eigen solution to the operator in order to obtain the dynamic modes [12]. This technique had several applications including controls and in vibrational systems, however, in the context of video-based sensing [13, 14]. In addition, modifications of the DMD algorithm were created, such as the optimized DMD, which uses an optimization approach to obtain the dynamic modes [15], or approaches that includes physics knowledge of the system [16].

This work proposes a comparison between different methods of order reduction using machine learning approaches, such as PCA, SVD and DMD. For that, different applications will be used such as sparse measurement obtained from accelerometers, a full-field measurement obtained from lased Doppler vibrometer (LDV) and video-based sensing.

Background

Dimension reduction techniques are usually known for machine learning applications. However, order reduction techniques can have similar procedure for other applications where the physical knowledge of the system is known. For example, modal analysis employs the eigen decomposition of the parameters of a governing equation (e.g. from a FEM) and can use a smaller number of mode shapes to describe the behavior of a structure. POD will have a similar mathematical procedure with measurements of a physical quantity. While for statistical or mathematical applications PCA and SVD will be used to decompose a set into smaller dimension. SVD for instance, can decompose an initial matrix X into two unitary matrices and a scalar as presented in Equation (1).

$$X \approx U\Sigma V^T \tag{1}$$

Where, U and V are unitary matrices and Σ is a rectangular and diagonal matrix containing the singular values. Meanwhile, PCA and POD can use either SVD for the decomposition, or it can calculate the covariance matrix of the dataset X. Since the covariance matrix will be a square matrix, then the eigen decomposition can obtain the modes and values for the variation of the data. The covariance matrix can be calculated according to Equation (2).

$$\widehat{\Sigma} = \frac{1}{n}\sum_{i=1}^{n}(x_i - \overline{x})(x_i - \overline{x})^T \tag{2}$$

Where, $\widehat{\Sigma}$ is the covariance matrix of the dataset, $\overline{x}$ is the mean of the data. After computing the covariance matrix of the normalized dataset, the principal components will be given by its eigen solution. DMD works in a similar manner to PCA and SVD. However, instead of using either the dataset itself or the covariance matrix, it will calculate an $[A]$ matrix which will be a time invariant matrix computed based on the Koopman operator as shown in Equation (3) and the process to calculate the DMD modes can be seen in Figure 1.

$$X^{'} \approx AX \tag{3}$$

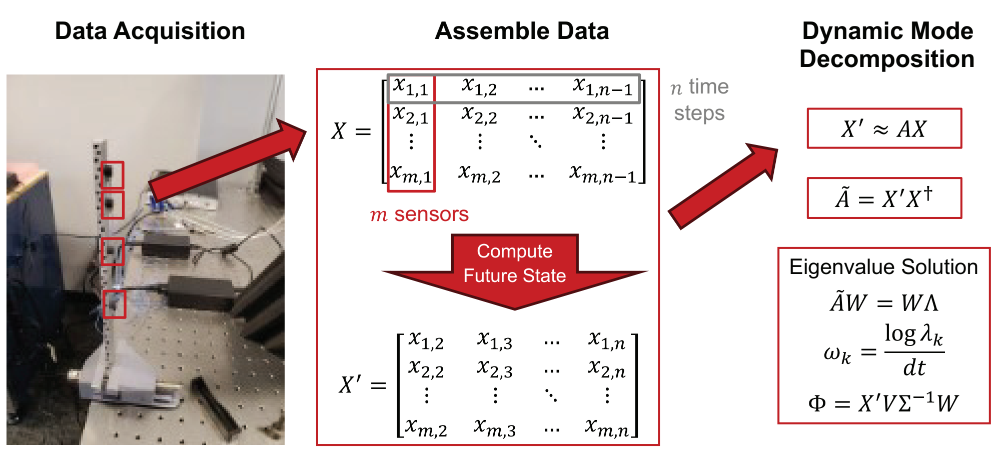

Fig. 1 Flowchart of DMD measurement and mode decomposition.

where, $X^{'}$ is the future state of the system, X is its current state and A the linear operator that predicts the future state based on the current state. Since DMD aims to reduce the order of the system, a low rank $\tilde{A}$ can be calculated based on the linear operator by applying SVD to the equation, as shown in Equation (4).

$$\tilde{A}{\approx}U^{T}AU = U^{T}X^{'}V\Sigma^{-1} \tag{4}$$

After calculating the low rank matrix $\tilde{A}$, the eigen decomposition will be computed following Equation (5).

$$\tilde{A}W{=}W\Lambda \tag{5}$$

where, W are the mode shapes associated with $\tilde{A}$ and Λ its eigenvalues. Finally, the DMD modes Φ can be calculated based on Equation (6).

$$\Phi{=}X^{'}V\Sigma^{-1}W \tag{6}$$

Later the signal reconstruction for each DMD mode is done by an exponential approximation as presented in Equation (7).

$$t_{DMD}{=}be^{\omega t} \tag{7}$$

t_{DMD} is the time reconstruction for each DMD mode, b is a scale factor based on the initial condition for each mode and sensor, and ω is the natural frequency calculated using the eigenvalue following Equation (8).

$$\omega_{k}{=}\frac{\log\lambda_{k}}{dt} \tag{8}$$

Given dt as the time-step between measurements. Finally, the time reconstruction from DMD is given by:

$$\hat{X}{\approx}\Phi \times t_{DMD} \tag{9}$$

Another existing approach for DMD is the optimized DMD. Instead of using linear algebra to calculate the DMD modes and frequencies, optimized DMD uses an iterative method by optimizing the following equation.

$$\min \left\| X - \Phi{\times}t_{DMD} \right\|_{F} \tag{10}$$

where $\|.\|_{F}$ is the Frobenius norm of a matrix and given by the square root of the matrix trace times its conjugate transposed. This approach optimizes the DMD reconstruction to the measured data, leading to a better time reconstruction if compared to the exact (original) DMD.

Experimental Setup

There were three experimental setups employed to compare the different order reduction techniques. Starting with an impact test in a cantilever beam, with a sparse measurement obtained from accelerometers. The setup can be seen in Figure 1, where four accelerometers were placed in the beam and the data collected consisted of 1,024 time-steps at 2.56kHz of sampling rate. The first two natural frequencies of the beam occurred at 48.6Hz and 435.3Hz.

For the second test, a cantilever plate was employed. For this case, the LDV scanned 133 points equally distributed thought the plate. The test collected a total of 50,000 timesteps at 100kHz of sampling rate. The excitation was a burst chirp for 50% of the testing time ranging from 100Hz to 10kHz. This testing setup meant to be employed as a full-field measurement of the structure, with higher number of measuring points, however, still with a smaller number of measured points than timesteps. The setup is presented in Figure 2a).

Finally, the last test was the same impact test from the cantilever beam, however, using a video-based measurement. No post processing was employed into the video, except for cropping the frame from a full HD resolution (1920x1080 pixels) to 400x1080 pixels. That was done to focus on the beam only and reduce the area of background. The measurement was performed at 960Hz of sampling rate and 2,000 points collected. The setup for the video-based sensing is shown in Figure 2b).

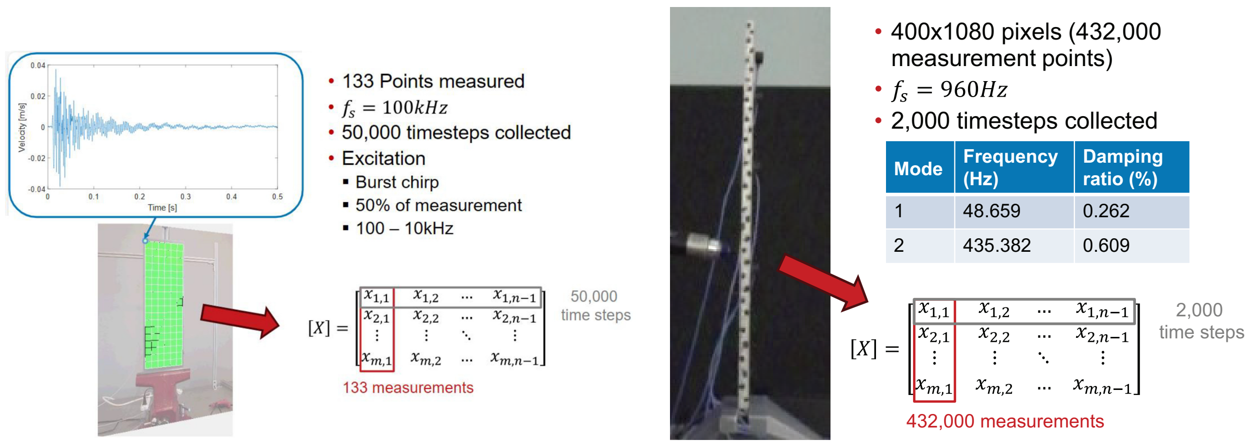

(a) (b)

Fig. 2 Experimental setup for the cantilever plate with LDV measurement (a) and cantilever beam with video-based measurement (b).

Results and Discussion

The results obtained by the reduction techniques will be presented by comparing each result of PCA, exact DMD and optimized DMD for each case. Starting with the results for the cantilever beam, which is a sparse measurement with only four accelerometers. The PCA results for the cantilever beam are presented in Figure 3 below.

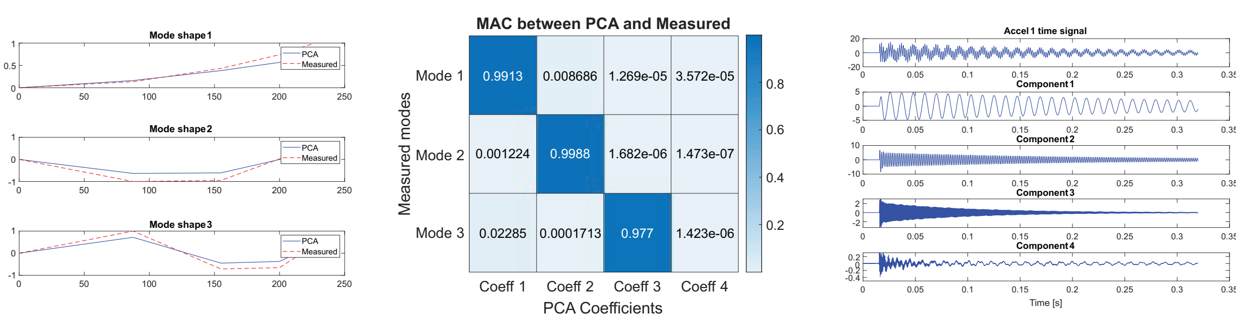

(a) (b) (c)

Fig. 3 Results of PCA to the cantilever beam, principal components compared to the mode shapes (a), MAC between the principal components and measured mode shapes (b) and time estimation for each component (c).

For the impact test, the highest variation of the data occurs based on the mode shapes of the structure, leading to a good correlation between the measured modes and principal components coefficients. As shown in Figure 3b) the MAC for the first three mode shapes are above 95% and the time estimation presented in (c) has a similar behavior, going from the low frequency sine wave to a high frequency one, with the last reconstruction having a behavior similar to noise. When applying exact DMD with sparse sensing, the mode shape estimation will also have good accuracy compared to the ones obtained by measurement for both mode shapes computed, as shown in Figure 4. However, DMD approximates the motion of the system using an exponential function. In order to obtain the oscillatory motion of the system, the eigenvalues computed will be composed of complex values. Therefore, four DMD modes can obtain only two of the real mode shapes of the beam as it can be seen in Figure 4b).

In addition, while exact DMD estimates modes well, its natural frequencies and time reconstruction have low accuracy. Figure 4c) presents each modal response, considering the small number of measurements, some of the eigenvalues obtained will be real values, leading to an exponential instead of an oscillatory behavior. Furthermore, the complex eigenvalues obtained possessed a high frequency and high damping ratio, leading to a small oscillation in the time domain, as shown in the two top plots of Figure 4c).

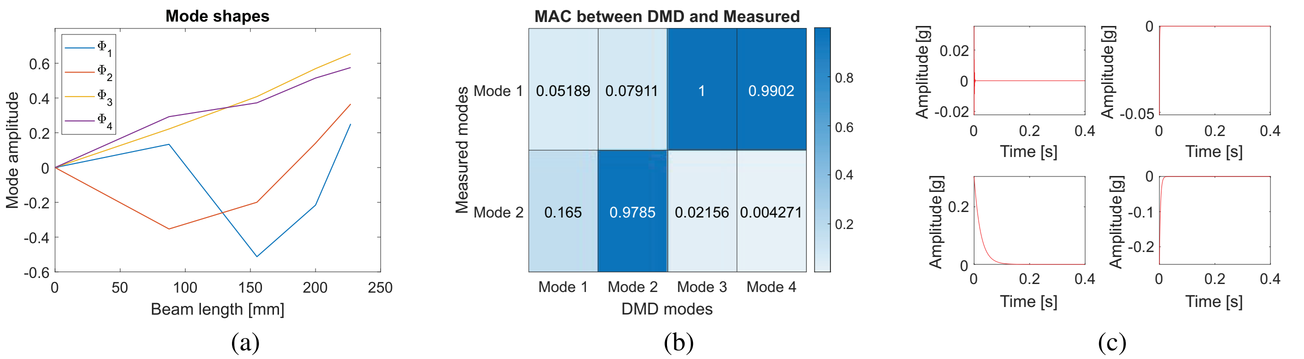

Fig. 4 Mode shape estimation (a) and MAC comparison (b) between exact DMD and measurement and time reconstruction for each mode (c).

Meanwhile, when applying optimized DMD on the dataset, the optimization algorithm focuses on the time reconstruction, as described in Equation (10). Therefore, the time estimation obtained will be better compared to the exact DMD as shown in Figure 5.

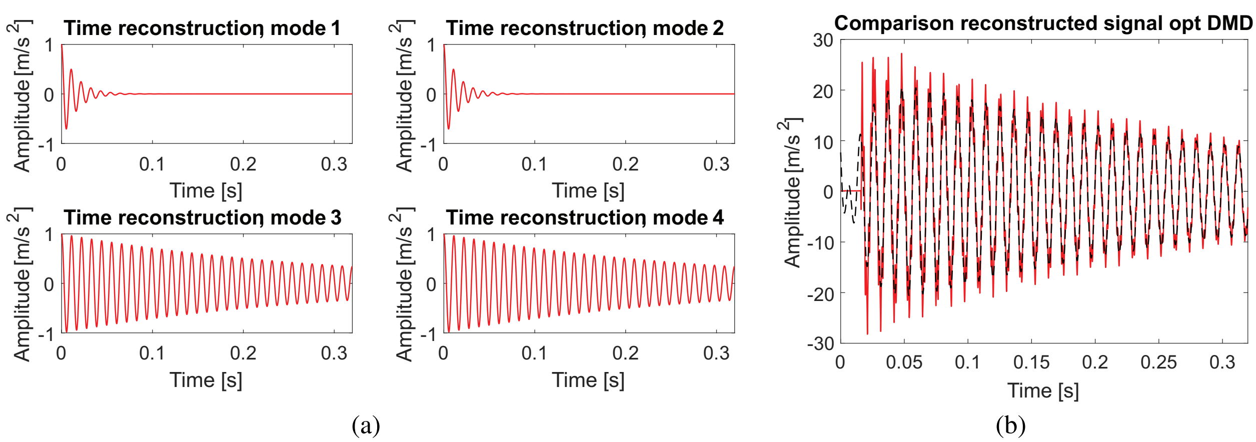

Fig. 5 Time estimation for each mode shape (a) and signal reconstruction (b) using optimized DMD.

In this case, modes 3 and 4 behave similarly to a modal response, and the signal reconstruction will have a better accuracy than the previous model. However, to obtain a good time reconstruction, the eigenvalues estimated are in a similar frequency range, as shown in Figure 6b). Since the natural frequency at 93.5Hz possesses the highest energy, the DMD estimation obtained the frequencies around the natural frequency estimation. Thus, only the first mode shape was extracted. The results of PCA applied to the cantilever plate having a full-field measurement using LDV is presented in Figure 7 as follows.

As shown in Figure 7a), most of the variation of the data happens in the first 20 components. Therefore, only 20 out of the 133 components would be able to reconstruct the original signal with a small error. However, since the forced vibration has different amplitude for different frequencies, it would be challenging to obtain the natural frequencies of the system based on the obtained parameters. In addition, since the order of the principal components are unknown, then the modes obtained can be from any natural frequency as it can be seen in (b) and (c). Meanwhile, when applying exact DMD to the plate, more mode shapes can be estimated, however, only when decomposing all 133 possible modes that some of the main natural frequencies are obtained.

Figure 8a) has the eigenvalues estimated for the plate, however, the eigenvalues are estimated from the highest frequency to the lowest and all frequencies are above 50Hz, avoiding some of the first mode shapes of the plate, such as the first bending mode at around 5∼6Hz. In addition, in (b), the time reconstruction for two nodes is given. Even using more than 100 mode shapes for the estimation, the estimation does not look like the measured signal (due to the difference they could not be plotted together, and the estimated signal would be too small and not visible). Finally, (c) presents the DMD mode at 268Hz, which has a similar behavior to a high-frequency mode shape.

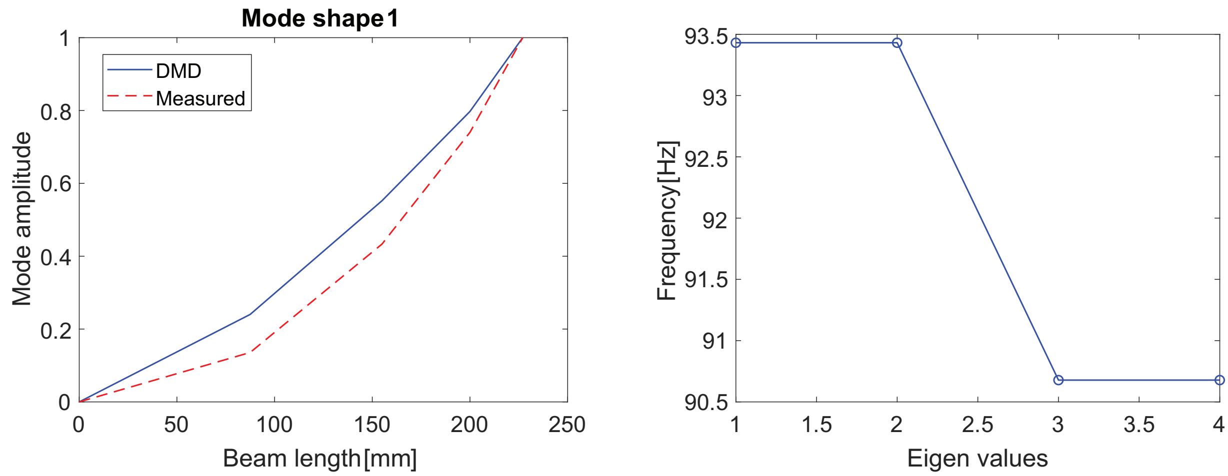

(a) (b)

Fig. 6 Mode shape (a) and natural frequencies (b) estimations using optimized DMD.

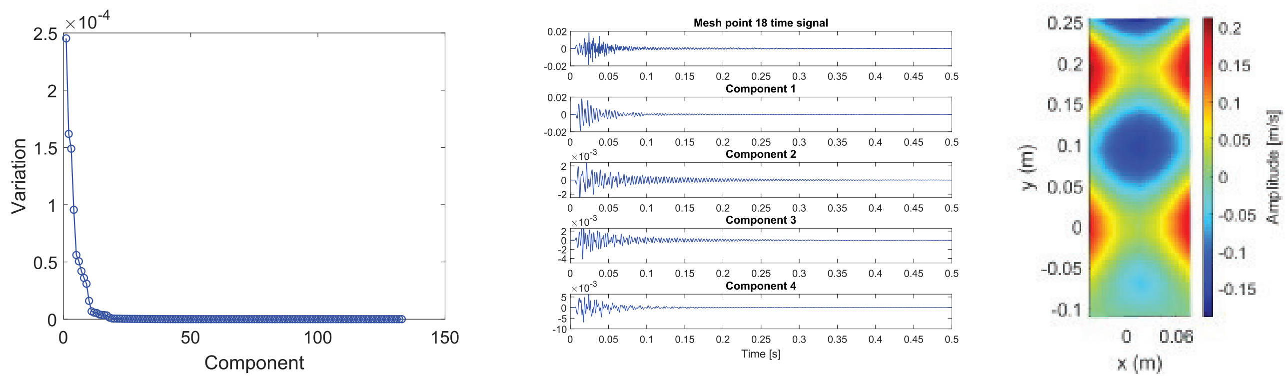

(a) (b) (c)

Fig. 7 Principal components (a), time reconstruction for each component (b) and first mode estimation (c) for PCA applied to the cantilever plate.

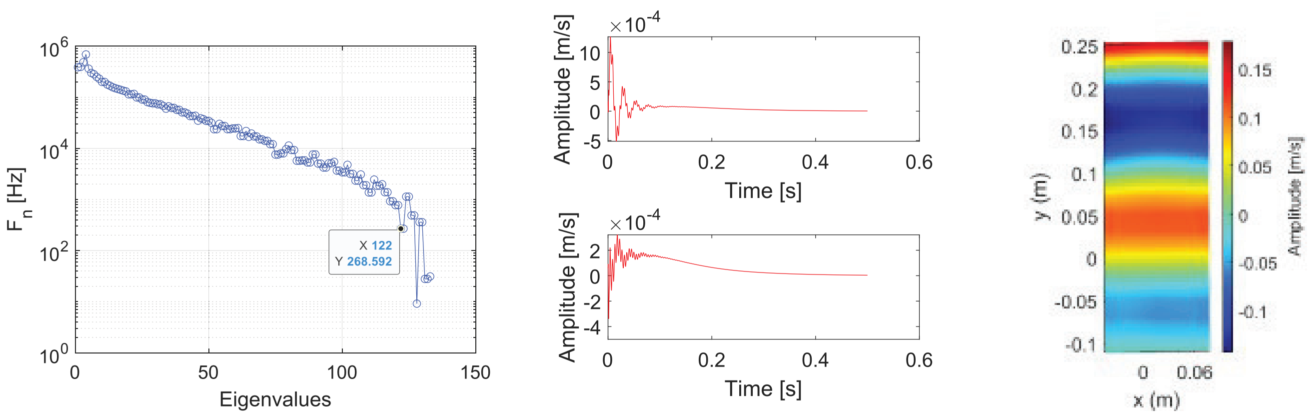

(a) (b) (c)

Fig. 8 Natural frequencies obtained from eigenvalues (a), time reconstruction (b) and mode shape estimation at 268Hz (c) using exact DMD.

When employing the same dataset into the optimized DMD algorithm, although the time for computing the correct answer is much higher than when using exact DMD, it requires a much lower number of eigenvalues to perform a good time reconstruction of the time signal. In Figure 9a) the estimated frequencies for the first 20 modes are presented. Similarly to the previous example, the eigenvalues are computed in pairs due to being estimated as a complex value. Using only 20 eigenvalues will give the TRAC shown in (b), in which most of the values are above 80% of signal reconstruction. The only exceptions are near the base of the plate, where the boundary condition causes low signal amplitude, and in the location where the shaker is positioned (which has around 60% reconstruction). Finally, the lowest frequency mode is presented in (c). This mode shape has a corresponding frequency of 5.6Hz which is similar to the real mode shape obtained by the LDV measurement. In addition, the first mode resembles a bending mode shape with values in the base close to zero and the highest value near the top of the plate.

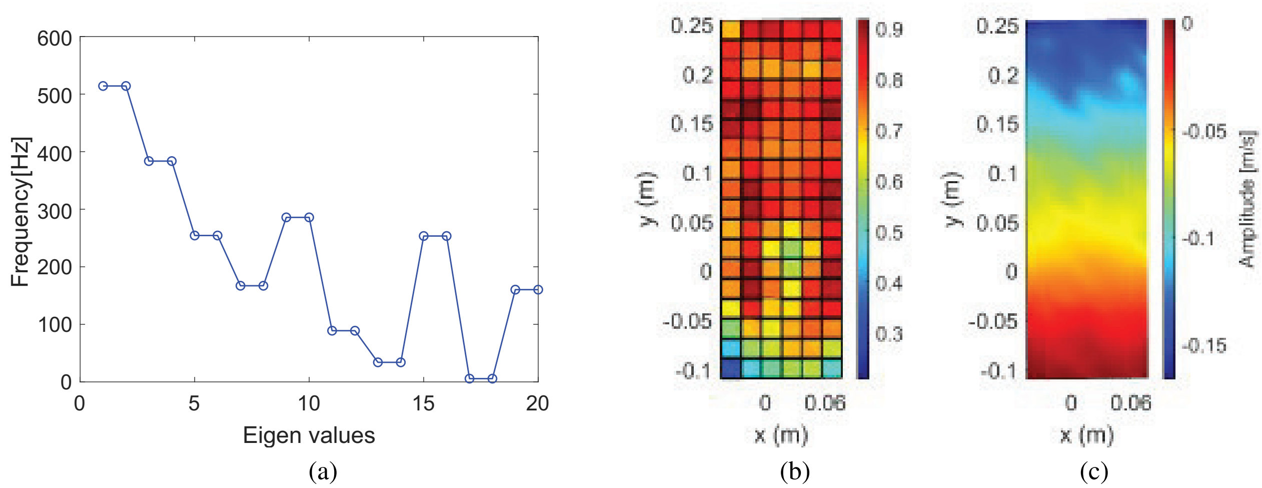

Fig. 9 Estimated natural frequencies (a), TRAC (b) and mode shape estimation at 5.6Hz (c) using optimized DMD.

Finally, PCA was employed for video-based datasets, for this case, the video of the cantilever beam was used, the image having 400x1080 pixels will give more than 400 thousand measure points while 2000 timesteps were recorded. For the application of PCA into the video-based data the results are presented in Figure 10 as follows.

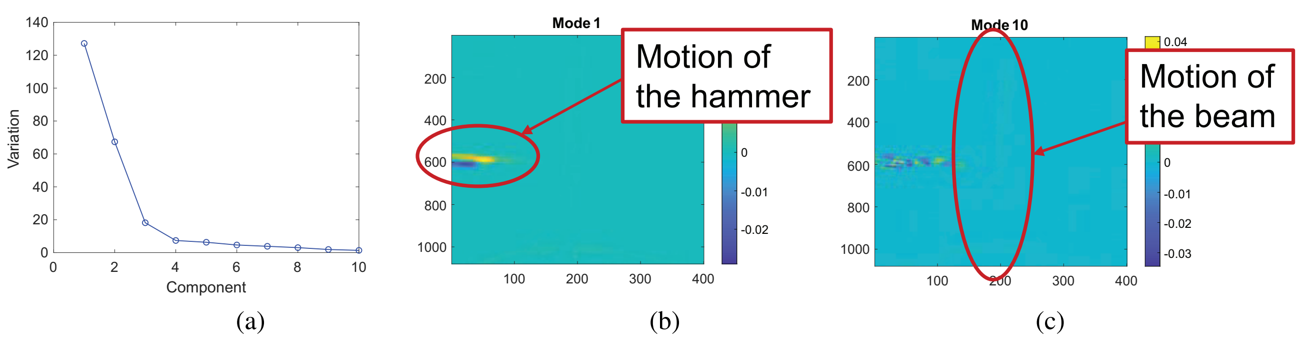

Fig. 10 Principal components (a), first mode reconstruction (b) and 10^{th} mode reconstruction (c) for PCA applied to video-based data.

Similarly to the cantilever plate case, most of the variation of the data happens on the first 10 components. However, for this case, the most variation of the data occurs on the transient motion from the hammer hitting the cantilever beam. Therefore, the modes obtained are similar to the ones presented on Figure 10b) and (c) with the mode only showing the motion of the hammer. Only after 10 modes it is possible to slightly see some motion of the beam itself. However, due to the natural frequencies to be unknown it is difficult to predict which mode will have any beam behavior. In addition, after the 10^{th} mode, the noise of the video starts to appear in the components as well, making it difficult to obtain the vibrational signal alone.

In terms of computational cost, PCA can compute all 2,000 modes from the data, having a similar time consumption from exact DMD. However, the optimized DMD has a much higher computational time required, allowing the usage of 40 dynamic modes. While, when employing exact DMD, 500 eigenvalues were computed, and the time of calculation was still considerably smaller than using optimized DMD. In addition, with 500 eigenvalues for the approximation a good time reconstruction could be performed.

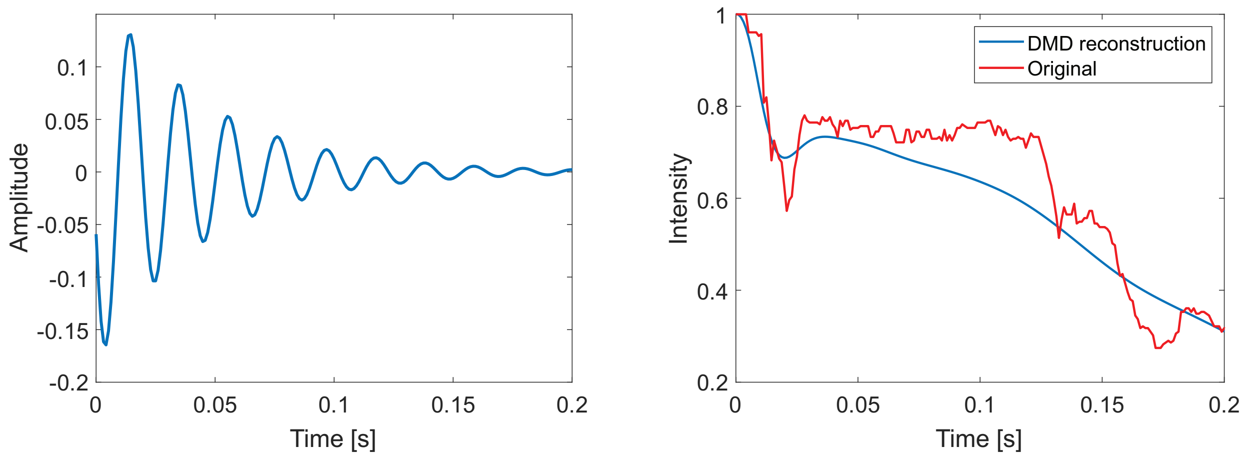

(a) (b)

Fig. 11 Time estimation for first mode shape of the beam (a), time reconstruction for an arbitrary pixel in the video (b) using exact DMD.

Figure 11a) presents the time response of the first DMD mode of the beam, while (b) shows the time reconstruction (in blue) of an arbitrary pixel. Since the measurement is given by the pixel intensity the intensity will only have a sine wave behavior in the edges of the beam, while most of the background will have only a noisy measurement.

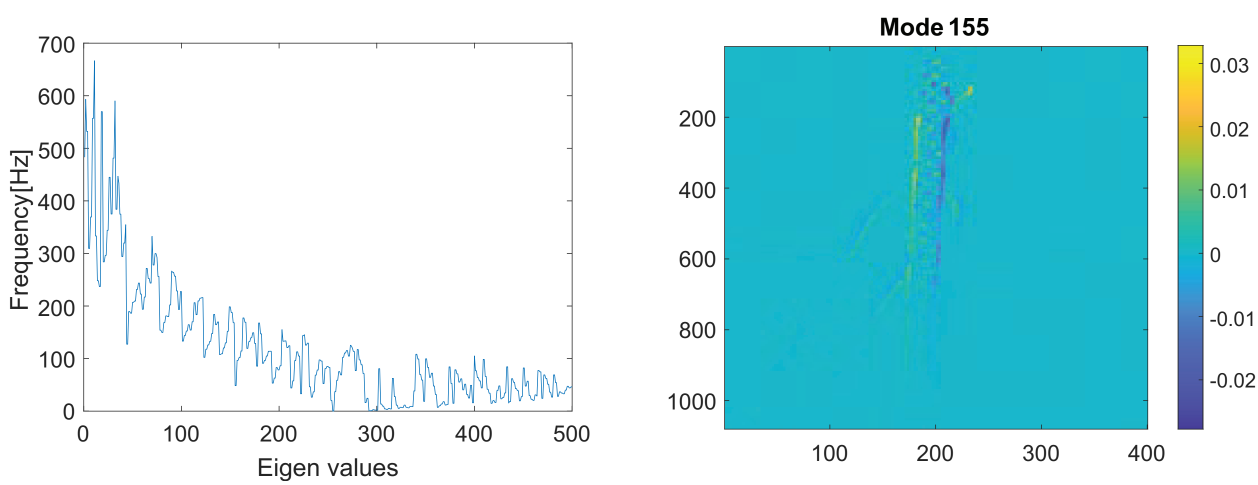

(a) (b)

Fig. 12 Eigenvalues (a) and first mode shape (b) of the beam using exact DMD in video-based data.

Figure 12a) shows the estimated frequencies from the eigenvalues. However, most of the measurements obtained in the video will be either noise floor measurements (background) or transient motion (such as the hammer moving to hit the beam). There will be eigenvalues corresponding to many frequencies. Then only the DMD mode which is equivalent to the natural frequency of the beam will be correctly identified, as in (b).

When applying the same dataset to optimized DMD, a smaller number of eigenvalues must be used to describe the system dynamics. However, since the dataset is large due to the number of measurements, the time consumption is considerably higher. Figure 13a) shows the eigenvalues obtained from optimized DMD when solving for 40 DMD modes. Since most of the background of the video is noise measurement, then many of the eigenvalues estimated were in low frequency (20Hz and below). However, since the first bending mode of the beam has a high energy level, then using 40 components is enough to obtain the bending mode, which is presented in (b) and now is the first mode of the model.

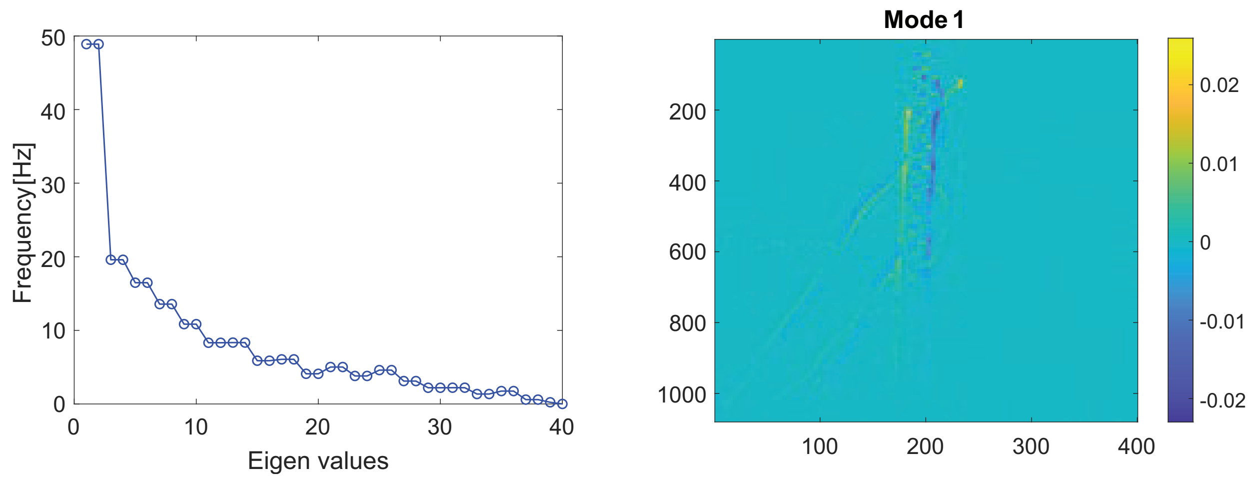

(a) (b)

Fig. 13 Eigenvalues (a) and first mode shape (b) of the beam using optimized DMD in video-based data.

When observing the time reconstruction of the original signal, Figure 14a) presents the time reconstruction for the first mode shape at 48.9Hz. While (b) shows the TRAC for all the pixels in the video. Notice that the TRAC is higher than 96% for all the pixels available, having then a very good time reconstruction for the vibration of the beam, as well as the transient motion of the hammer and the background noise.

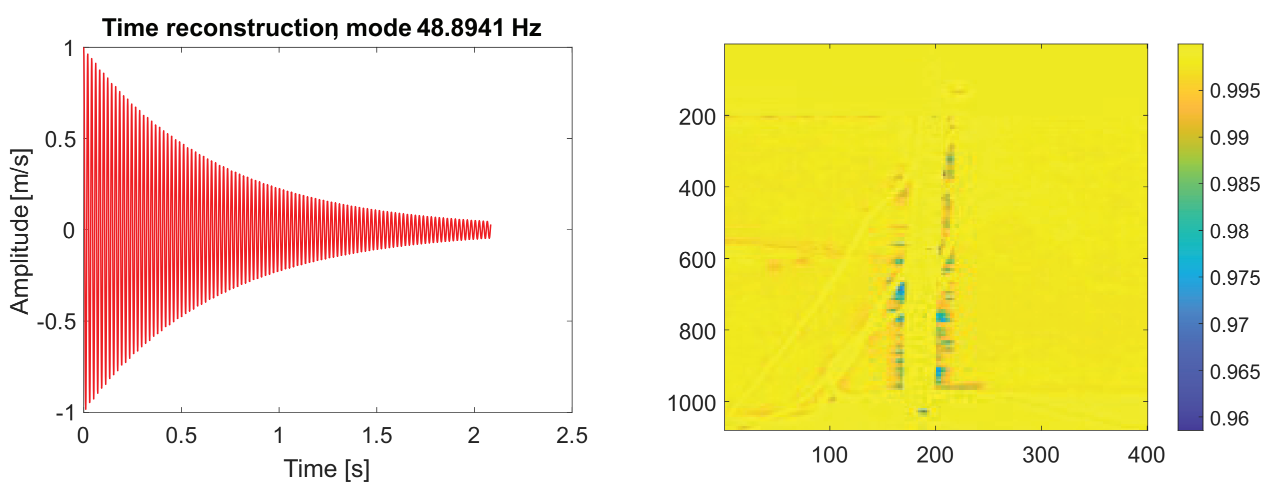

(a) (b)

Fig. 14 Response estimation for the first DMD mode (a) and TRAC for all the pixels (b).

In summary, when employing PCA for vibrational systems, it was observed that its performance gets better for time reconstruction, since it is only a transformation in the basis of the measurement. However, the mode shape reconstruction will be feasible only for simple systems where it is known that the modes of interest have the most excitation during the test. Meanwhile, it was observed that the exact DMD will perform better for high-dimensional datasets. In other words, generally for datasets that possess more measuring points than timesteps, e.g. video-based data, will lead to a better DMD implementation. For low dimensional data, such as accelerometer and LDV measurements, there will be too many real eigenvalues, which will reduce the accuracy of the signal reconstruction. Meanwhile, optimized DMD has a better time and frequency estimation for all systems, and it requires a smaller number of measurements to be effective. For instance, with 20-40 eigenvalues it was able to reproduce with good accuracy the measurements from the video data and LDV measurements, not to mention the feasibility on dealing with sparse measurements, such as accelerations at discrete locations. However, due to the limited number of sensors, it will only be able to obtain the first mode shape of the system. The limitation of exact DMD lies in the computational and time cost to perform the calculations. For example, the LDV data has a small number of sensors, but the number of timesteps was large, leading to a large computational time. Similarly, the video-based data had a small number of timesteps, but a large number of pixels, leading to a high computational cost.

Conclusion

This work presents a comparison study between different data-driven techniques used for order reduction. The applications selected were based on different measurement equipment, that can obtain sparse or full-field measurement. In addition, when performing full-field measurement, video-based data was also employed leading to a dataset with more measuring points than time-steps obtained. Optimized DMD had overall a better estimation for all applications; while having a good accuracy for signal reconstruction it also maintains the physical information of the system. However, its high computational cost, might not be feasible to high-dimensional data, such as video-based.

For future research directions, other variations of both DMD and other traditional dimension reduction techniques could be explored, such as physics-informed DMD or t-SNE. In addition, studies on subsystems and nonlinear systems could be implemented using the data-driven approaches presented.

Acknowledgments This work is supported by the Department of Energy Kansas City National Security Campus Managed by Honeywell under contract # N000510678. NSC-614-5662 10/2024. Unclassified Unlimited Release.

References

1. S. Wold, K. Esbensen, and P. Geladi, “Principal component analysis,” Chemometrics and intelligent laboratory systems, vol. 2, no. 1–3, pp. 37–52, 1987.
2. M. E. Wall, A. Rechtsteiner, and L. M. Rocha, “Singular value decomposition and principal component analysis,” in A practical approach to microarray data analysis: Springer, 2003, pp. 91–109.
3. C. Wu, Y. Liang, W. Lin, H. Lee, and S. Lim, “A note on equivalence of proper orthogonal decomposition methods,” Journal of Sound and Vibration, vol. 265, no. 5, pp. 1103–1110, 2003.
4. G. Kerschen and J.-C. Golinval, “Physical interpretation of the proper orthogonal modes using the singular value decomposition,” Journal of Sound and vibration, vol. 249, no. 5, pp. 849–865, 2002.
5. P. J. Schmid, “Data-driven and operator-based tools for the analysis of turbulent flows,” in Advanced Approaches in Turbulence: Elsevier, 2021, pp. 243–305.
6. E. Aoki, C. T. do Cabo, Z. Mao, Y. Ding, and S. Ozharar, “Vibration-Based Status Identification of Power Transmission Poles,” IFAC-PapersOnLine, vol. 55, no. 27, pp. 214–217, 2022.
7. R. J. Allemang, A. W. Phillips, and M. R. Allemang, “Application of principal component analysis methods to experimental structural dynamics,” in Structural Dynamics, Volume 3: Proceedings of the 28th IMAC, A Conference on Structural Dynamics, 2010, 2011: Springer, pp. 477–498.
8. H.-W. Ma, Y.-Z. Lin, and Z.-H. Nie, “Physical interpretation of principal component analysis for structural dynamics through string vibration,” International Journal of Structural Stability and Dynamics, vol. 19, no. 09, p. 1950109, 2019.
9. P. J. Schmid, “Dynamic mode decomposition of numerical and experimental data,” Journal of fluid mechanics, vol. 656, pp. 5–28, 2010.
10. J. H. Tu, “Dynamic mode decomposition: Theory and applications,” Princeton University, 2013.
11. J. N. Kutz, S. L. Brunton, B. W. Brunton, and J. L. Proctor, Dynamic mode decomposition: data-driven modeling of complex systems. SIAM, 2016.
12. S. L. Brunton, “Notes on Koopman operator theory,” Universität von Washington, Department of Mechanical Engineering, Zugriff, vol. 30, 2019.
13. J. L. Proctor, S. L. Brunton, and J. N. Kutz, “Dynamic mode decomposition with control,” SIAM Journal on Applied Dynamical Systems, vol. 15, no. 1, pp. 142–161, 2016.
14. N. A. Valente, C. T. do Cabo, Z. Mao, and C. Niezrecki, “Dynamic Mode Decomposition for Resonant Frequency Identification of Oscillating Structures,” in Society for Experimental Mechanics Annual Conference and Exposition, 2023: Springer, pp. 155–162.
15. T. Askham and J. N. Kutz, “Variable projection methods for an optimized dynamic mode decomposition,” SIAM Journal on Applied Dynamical Systems, vol. 17, no. 1, pp. 380–416, 2018.
16. P. J. Baddoo, B. Herrmann, B. J. McKeon, J. Nathan Kutz, and S. L. Brunton, “Physics-informed dynamic mode decomposition,” Proceedings of the Royal Society A, vol. 479, no. 2271, p. 20220576, 2023.